Original Article

Performance assessment of an artificial intelligence-based coronary artery calcium scoring algorithm in non-gated chest CT scans of different slice thickness

Kejie Yin[1#], Wenping Chen[1#], Guochu Qin[1#], Jing Liang[1], Xue Bao[2], Hongming Yu[1], Hui Li[1], Jianhua Xu[3], Xingbiao Chen[4], Yujie Wang[5], Rock H. Savage[6], U. Joseph Schoepf[6], Dan Mu[1,3], Bing Zhang[1]

[1]Department of Radiology, Drum Tower Hospital, Medical School of Nanjing University, Nanjing, China; [2]Department of Cardiology, Drum Tower Hospital, Medical School of Nanjing University, Nanjing, China; [3]Department of Radiology, Yizheng Hospital of Nanjing Drum Tower Hospital Group, Yizheng, China; [4]Clinical Science, Philips Healthcare, Shanghai, China; [5]Department of Radiology, Nanjing Drum Tower Hospital Clinical College of Jiangsu University, Nanjing, China; [6]Department of Radiology and Radiological Science, Division of Cardiovascular Imaging, Medical University of South Carolina, Charleston, SC, USA

Contributions: (I) Conception and design: D Mu, K Yin, UJ Schoepf, G Qin; (II) Administrative support: D Mu, B Zhang, G Qin; (III) Provision of study materials or patients: K Yin, W Chen, G Qin; (IV) Collection and assembly of data: K Yin, W Chen, J Liang, H Yu, H Li, J Xu, Y Wang, RH Savage; (V) Data analysis and interpretation: K Yin, X Bao, X Chen; (VI) Manuscript writing: All authors; (VII) Final approval of manuscript: All authors.

[#]These authors contributed equally to this work as co-first authors.

Correspondence to: Dan Mu, MD. Department of Radiology, Drum Tower Hospital, Medical School of Nanjing University, No. 321 Zhongshan Road, Nanjing 210008, China; Department of Radiology, Yizheng Hospital of Nanjing Drum Tower Hospital Group, Yizheng, China. Email: mudan118@126.com; U. Joseph Schoepf, MD. Department of Radiology and Radiological Science, Division of Cardiovascular Imaging, Medical University of South Carolina, 25 Courtenay Drive, Charleston, SC 29425-2260, USA. Email: schoepf@musc.edu.

Background: The coronary artery calcium score (CACS) has been shown to be an independent predictor of cardiovascular events. The traditional coronary artery calcium scoring algorithm has been optimized for electrocardiogram (ECG)-gated images, which are acquired with specific settings and timing. Therefore, if the artificial intelligence-based coronary artery calcium score (AI-CACS) could be calculated from a chest low-dose computed tomography (LDCT) examination, it could be valuable in assessing the risk of coronary artery disease (CAD) in advance, and it could potentially reduce the occurrence of cardiovascular events in patients. This study aimed to assess the performance of an AI-CACS algorithm in non-gated chest scans with three different slice thicknesses (1, 3, and 5 mm).

Methods: A total of 135 patients who underwent both LDCT of the chest and ECG-gated non-contrast enhanced cardiac CT were prospectively included in this study. The Agatston scores were automatically derived from chest CT images reconstructed at slice thicknesses of 1, 3, and 5 mm using the AI-CACS software. These scores were then compared to those obtained from the ECG-gated cardiac CT data using a conventional semi-automatic method that served as the reference. The correlations between the AI-CACS and electrocardiogram-gated coronary artery calcium score (ECG-CACS) were analyzed, and Bland-Altman plots were used to assess agreement. Risk stratification was based on the calculated CACS, and the concordance rate was determined.

Results: A total of 112 patients were included in the final analysis. The correlations between the AI-CACS at three different thicknesses (1, 3, and 5 mm) and the ECG-CACS were 0.973, 0.941, and 0.834 (all $P<0.01$), respectively. The Bland-Altman plots showed mean differences in the AI-CACS for the three thicknesses of −6.5, 15.4, and 53.1, respectively. The risk category agreement for the three AI-CACS groups was 0.868, 0.772, and 0.412 (all $P<0.01$), respectively. While the concordance rates were 91%, 84.8%, and 62.5%, respectively.

Conclusions: The AI-based algorithm successfully calculated the CACS from LDCT scans of the chest, demonstrating its utility in risk categorization. Furthermore, the CACS derived from images with a slice thickness of 1 mm was more accurate than those obtained from images with slice thicknesses of 3 and 5 mm.

Keywords: Cardiovascular disease; computed tomography (CT); artificial intelligence (AI); coronary artery disease (CAD)

Submitted Feb 05, 2024. Accepted for publication Jul 05, 2024. Published online Jul 24, 2024.
doi: 10.21037/qims-24-247
View this article at: https://dx.doi.org/10.21037/qims-24-247

Introduction

Cardiovascular diseases are the leading cause of death globally, ranking first in the global disease burden (1). Among cardiovascular diseases, coronary artery disease (CAD) is the "number one killer" (2,3). Coronary artery atherosclerosis is the fundamental pathological basis of CAD and coronary artery calcium (CAC) is an early sign of coronary atherosclerosis and is closely associated with the incidence rate of CAD (3,4).

The coronary artery calcium score (CACS) is a quantitative index of CAC. The CACS has been shown to be an independent predictor of cardiovascular events, particularly in asymptomatic middle-risk populations (5). The early and accurate assessment of CAC is crucial for mitigating increased risk of CAD (6). The Agatston score, which was originally proposed by Agatston *et al.* (7) and is obtained from electrocardiogram (ECG)-gated computed tomography (CT), remains the most widely used method for measuring the CACS. The categorization of patients into CAD risk categories based on the CACS can be used to guide treatment (8).

Public awareness of health examinations is increasing and non-gated low-dose computed tomography (LDCT) of the chest has become a widely used screening method for lung diseases (9,10); however, ECG-gated CT is not typically included as part of routine health examinations. Due to the presence of cardiac motion artifacts, traditional methods for calculating the CACS of non-gated chest CT may not be accurate (11). The traditional CACS algorithm has been optimized for ECG-gated images, which are acquired with specific settings and timing. However, some studies have reported a high correlation between ECG-gated CT and non-gated LDCT scans of the chest in the Agatston score (12-14). Therefore, if the CACS could be calculated from a LDCT examination of the chest, it could be valuable in assessing the risk of CAD in advance, and it could potentially reduce the occurrence of cardiovascular events in patients.

With continued advances in science and technology, artificial intelligence (AI) has been applied to an increasing number of medical fields. Through the use of deep-learning algorithms on computers, AI has the potential to significantly enhance work efficiency while substantially reducing the workload of humans (6,14-17). The integration of AI technology has the potential to appropriately mitigate the impact of cardiac motion artifacts on the calculation of the CACS from non-gated chest CT scans. Artificial intelligence-based coronary artery calcium score (AI-CACS) algorithms on ECG-gated cardiac CT (18,19) and non-gated chest CT (13,20-24) have been both developed, enabling the rapid evaluation of the CACS for a large number of patients.

Thus, this study sought to assess the consistency of the CACS calculated from ECG-gated and non-gated CT scans from routine health examinations and to evaluate the feasibility of assessing CAD risk using the CACS from LDCT with an AI-CACS algorithm. We present this article in accordance with the STROBE reporting checklist (available at https://qims.amegroups.com/article/view/10.21037/qims-24-247/rc).

Methods

Patients

This prospective study was approved by the Institutional Ethics Committee of the Drum Tower Hospital, Medical School of Nanjing University (No. 2022-547-01), and informed consent was obtained from all the patients. The study was conducted in accordance with the Declaration of Helsinki (as revised in 2013). From July 2022 to March 2023, patients suspected of CAD were enrolled in this study. These patients underwent sequential non-gated LDCT of

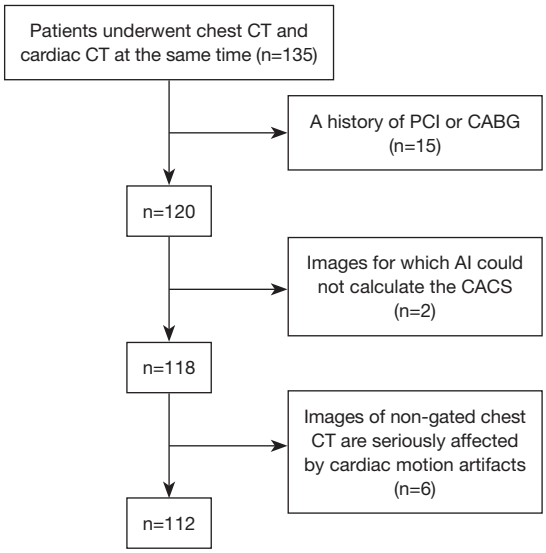

Figure 1 Flow chart of patient selection. CT, computed tomography; CACS, coronary artery calcium score; PCI, percutaneous coronary intervention; CABG, coronary artery bypass grafting; AI, artificial intelligence.

the chest and ECG-gated non-enhanced cardiac CT scans. Patients were excluded from the study if they met any of the following exclusion criteria: (I) had a history of transluminal percutaneous coronary intervention, coronary artery bypass grafting, or insertion of other metal implants; and/or (II) their images from the non-gated chest CT scans had serious artifacts due to cardiac motions. For more details about patient selection, see *Figure 1*.

CT scanning and CACS calculations

All the CT datasets were acquired using a third-generation dual-source CT system (SOMATOM Force, Siemens Healthineers, Forchheim, Germany). Participants underwent three types of scans; that is, a non-gated LDCT of the chest, followed by an ECG-gated non-contrast cardiac CT, and coronary computed tomography angiography (CTA). For details of scan parameters, see *Table 1*.

The volume computed tomography dose index ($CTDI_{vol}$) and dose length product (DLP) of chest CT and ECG-gated non-contrast cardiac CT scans were recorded. The effective dose (ED) was calculated using the following formula: ED (mSv) = DLP × k, where k was the chest (heart) ED conversion factor, with k = 0.014 $mSv \cdot mGy^{-1} \cdot cm^{-1}$ (25).

Following the Agatston convention, the CACS was calculated when the CT value was ≥130 Hounsfield units (HU) and the area was >1 mm^2 (7,26). The ECG-gated non-enhanced cardiac images were transferred to an advanced workstation (Intellispace Portal V9; Philips Healthcare, Best, The Netherlands) for the semi-automated CACS calculation. The coronary calcification analysis was performed by an experienced radiologist with 5 years of experience in cardiac CT imaging. The calculated CACS for each patient was considered as the reference in this study.

AI-CACS software (CACScoreDoc version 6.11, ShuKun Technology, Beijing, China) was developed and implemented to automatically calculate the CACS based on the chest CT images. In our process, the three-dimensional Retina-Unet deep convolutional neural network was used to segment the calcified lesions in the coronary area. Similar to other segmentation networks, the main structure was a fully convolutional feature pyramid network. Next, a detection branch and a segmentation branch were applied as the whole supervision function (*Figure 2*). A description of the AI-CACS model is provided in the Appendix 1. The non-gated chest CT images were uploaded to the AI-CACS software for CACS calculation with slice thicknesses of 1, 3, and 5 mm, respectively.

Risk category performance of the AI-CACS software

The correlations between the CACS (1-mm AI-CACS, 3-mm AI-CACS, 5-mm AI-CACS, and ECG-CT AI-CACS) obtained by the AI-CACS software and the ECG-CT CACS were studied, respectively. Based on the CACS, the patients were stratified into the following four different risk categories: CACS 0, very low risk of CAD; CACS 1–100, low risk of CAD; CACS 101–400, moderate risk of CAD; and CACS >400, high risk of CAD (22).

Statistical analysis

The statistical analysis was performed with SPSS software (version 27, IBM, Armonk, NY, USA) and MedCalc software (version 22.013, Ostend, Belgium). The continuous data are presented as the mean ± standard deviation, and the categorical variables are presented as the frequency and percentage. Because not all data adheres to a normal distribution or exhibits squared deviations, Wilcoxon tests were employed to compare the CACSs obtained by the AI-CACS software (1-mm AI-CACS, 3-mm AI-CACS, 5-mm

Table 1 Three types of scan parameters

Scan type	Chest CT	Non-contrast cardiac CT	Coronary CTA
Scan range	From the apex of the lungs to the lung bases	From the carina to the apex of the heart	From the carina to the apex of the heart
Tube voltage	Modulated tube voltage (70–120 kV)	120 kVp	Modulated tube voltage (80–120 kV)
Tube current	Modulated tube current with a reference value of 80 mAs	Modulated tube current with a reference value of 85 mAs	Modulated tube current (300–700 mAs)
Collimation (mm)	2×192×0.6	2×192×0.6	2×192×0.6
Gantry rotation time (s)	0.25	0.25	0.25
Field of view (mm)	350	155	155
Matrix	512×512	512×512	512×512
Slice width (mm)	1/3/5	3	0.75
Increment (mm)	1/3/5	1.5	0.5

CT, computed tomography; CTA, computed tomography artery.

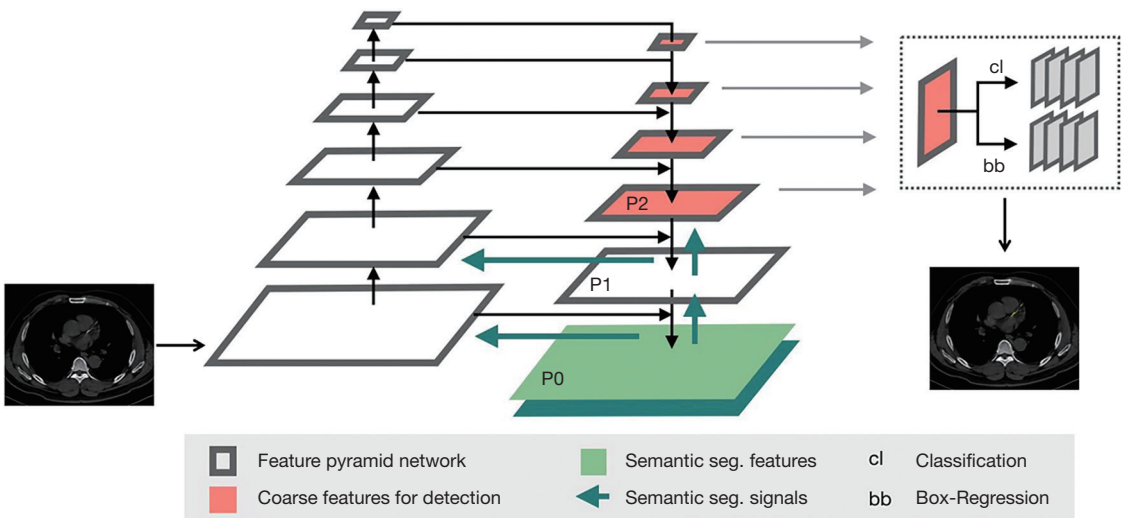

Figure 2 In our process, the three-dimensional Retina-Unet deep convolutional neural network was used to segment calcified lesions in the coronary area. Similar to other segmentation networks, the main structure was a fully convolutional feature pyramid network. ThNexten, a detection branch and a segmentation branch were applied as the whole supervision function.

AI-CACS) and the ECG-CT CACSs. A Bland-Altman analysis and Spearman correlation coefficients were used to evaluate agreement and correlation. The consistency of risk stratification was assessed with Kappa tests. A Kappa value (κ) of <0.4, 0.4–0.6, 0.6–0.8, and >0.8, indicated poor, moderate, good, and excellent agreement, respectively. A P value <0.05 was considered statistically significant.

Results

General information

A total of 112 patients were included in the study, of whom 74 were male and 38 were female. The patients had a mean age of 58.49±9.52 years (range, 37–78 years). *Table 2* shows the radiation dose of the three types of CT scans.

Table 2 CT radiation dose

Scan types	$CTDI_{vol}$ (mGy)	DLP (mGy·cm)	ED (mSv)
Chest	2.8±0.9	105.3±28.6	1.5±0.4
Cardiac non-contrast	2.6±0.7	35.7±14.3	0.5±0.2
Coronary CTA	18.7±8.5	303.5±156.7	4.2±2.2

Data are presented as mean ± standard. CT, computed tomography; $CTDI_{vol}$, volume computed tomography dose index; DLP, dose length product; ED, effective dose; CTA, computed tomography angiography.

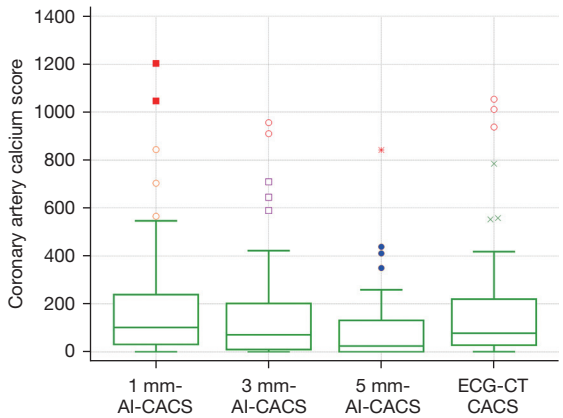

Figure 3 Box-and-Whisker plot showing the distribution of the coronary artery calcium scores of 1-mm AI-CACS, 3-mm AI-CACS, 5-mm AI-CACS, and ECG-CT CACS (data with a CACS of 0 were removed from the ECG-CT CACS group). The points, squares, crosses, or asterisks in the figure represent the CACS of the corresponding group of patients. AI, artificial intelligence; CACS, coronary artery calcium score; CT, computed tomography; ECG, electrocardiogram.

Table 3 Coronary artery calcium score

Groups	Coronary artery calcium score
1-mm AI-CACS	107.24±205.46
3-mm AI-CACS	85.33±174.73
5-mm AI-CACS	47.57±113.64
ECG-CT CACS	100.40±200.95

Data are presented as mean ± standard. AI-CACS, artificial intelligence-based coronary artery calcium score; ECG-CT CACS, electrocardiogram-gated computed tomography coronary artery calcium score.

CACS

There were no statistically significant differences between the 1-mm AI-CACS and ECG-CT CACS (107.24±205.46 *vs.* 100.40±200.95, P=0.085). Conversely, both the 3-mm AI-CACS and 5-mm AI-CACS were significantly lower than the reference ECG-CT CACS (85.33±174.73, 47.57±113.64; both P<0.001). For further details, see *Figure 3* and *Table 3*.

The correlations between the 1-mm AI-CACS, 3-mm AI-CACS, and 5-mm AI-CACS with ECG-CT CACS were strong (ρ=0.973 ,0.941, and 0.834; all P<0.001). The Bland-Altman plot revealed that the difference between the 1-mm AI-CACS and ECG-CT CACS was small [mean difference: −6.5, 95% confidence interval (CI): −95.0 to 81.9]. However, the difference between the 3-mm AI-CACS and ECG-CT CACS, as well as that between the 5-mm AI-CACS and ECG-CT CACS, were 15.4 (95% CI: −96.6 to 127.4), and 53.1 (95% CI: −187.8 to 294.0), respectively (*Figure 4*).

Agreement of risk categorization

In comparison with the ECG-CT CACS, the agreement of risk categories was excellent for the 1-mm AI-CACS group (κ=0.868), good for the 3-mm AI-CACS group (κ=0.772), and moderate for the 5-mm AI-CACS group (κ=0.412) (all P<0.001). More specifically, 91%, 84.8%, and 62.5% of the patients in the 1-mm AI-CACS, 3-mm AI-CACS and 5-mm AI-CACS groups were placed in the same category as they had been using the ECG-CT CACS, which served as the reference (*Tables 4-6*). Additionally, in comparison with the 1-mm AI-CACS, the agreement of risk categories was excellent for the 3-mm AI-CACS group (κ=0.769; P<0.001). Additionally, 85.6% of the patients in the 3-mm AI-CACS group were placed in the same category as they had been using the 1-mm AI-CACS (*Table 7*). In the three AI-CACS groups, the CACSs were more likely to be underestimated or overestimated when the patients were evaluated as low-risk [1–100] CAD patients (*Figures 5,6*). However, the CACSs of very few patients were overestimated in the 1 mm–AI-CACS groups (*Figure 7*).

Discussion

Numerous studies have suggested that CACS screening

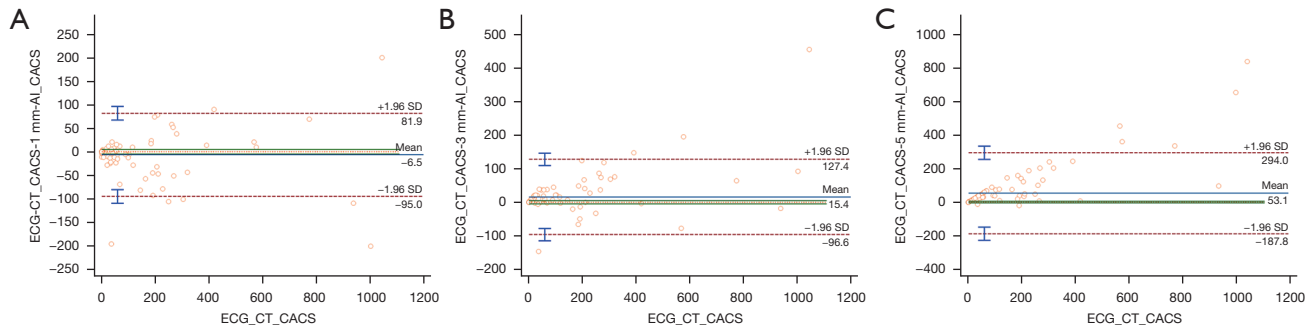

Figure 4 Bland-Altman plots showing the bias and 95% limits of agreement of red area. (A) 1-mm AI-CACS *vs.* ECG-CT CACS; (B) 3-mm AI-CACS *vs.* ECG-CT CACS; (C) 5-mm AI-CACS *vs.* ECG-CT CACS. AI, artificial intelligence; CACS, coronary artery calcium score; CT, computed tomography; ECG, electrocardiogram.

Table 4 Confusion matrices of risk categories between the 1-mm AI-CACS group and ECG-CT CACS group

1-mm AI-CACS	ECG-CT CACS, n				Total, n	Underestimation, n (%)	Overestimation, n (%)	Concordance, n (%)
	0	1–100	101–400	>400				
0	46	4	0	0	50	4 (8.0)	–	46 (92.0)
1–100	1	29	0	0	30	0	1 (3.3)	29 (96.7)
101–400	0	3	21	1	25	1 (4.0)	3 (12.0)	21 (84.0)
>400	0	0	1	6	7	–	1 (14.3)	6 (85.7)
Total	47	36	22	7	112	5 (4.5)	5 (4.5)	102 (91.0)

Kappa analysis κ=0.868, P<0.001; expressed as Spearman's correlation coefficient (ρ=0.973), P<0.001. AI-CACS, artificial intelligence-based coronary artery calcium score; ECG-CT CACS, electrocardiogram-gated computed tomography coronary artery calcium score.

Table 5 Confusion matrices of risk categories between the 3-mm AI-CACS group and ECG-CT CACS group

3-mm AI-CACS	ECG-CT CACS, n				Total, n	Underestimation, n (%)	Overestimation, n (%)	Concordance, n (%)
	0	1–100	101–400	>400				
0	47	13	0	0	60	13 (21.7)	–	47 (78.3)
1–100	0	22	2	0	24	2 (8.3)	0	22 (91.7)
101–400	0	1	20	1	22	1 (4.5)	1 (4.5)	20 (91.0)
>400	0	0	0	6	6	–	0	6 (100.0)
Total	47	36	22	7	112	16 (14.3)	1 (0.9)	95 (84.8)

Kappa analysis κ=0.772, P<0.001; expressed as Spearman's correlation coefficient (ρ=0.941), P<0.001. AI-CACS, artificial intelligence-based coronary artery calcium score; ECG-CT CACS, electrocardiogram-gated computed tomography coronary artery calcium score.

in asymptomatic populations could significantly reduce the incidence of adverse cardiovascular events (27-29). Our study showed the feasibility of calculating the CACS from chest CT scans of routine health examinations for individuals using an AI-based algorithm. The proposed deep-learning method in this study is feasible for the automatic quantification of the CACS in non-gated chest CT images of routine health examinations for individuals. The main findings from this study are as follows: (I) the automatic quantification of the CACS exhibited excellent correlation, consistency, and risk classification performance in non-gated chest CT images with slice thicknesses of

Table 6 Confusion matrices of risk categories between the 5-mm AI-CACS group and ECG-CT CACS group

5-mm AI-CACS	ECG-CT CACS, n				Total, n	Underestimation, n (%)	Overestimation, n (%)	Concordance, n (%)
	0	1–100	101–400	>400				
0	47	28	0	0	75	28 (37.3)	–	47 (62.7)
1–100	0	8	10	0	18	10 (55.6)	0	8 (44.4)
101–400	0	0	12	4	16	4 (25.0)	0	12 (75.0)
>400	0	0	0	3	3	–	0	3 (100.0)
Total	47	36	22	7	112	28 (25.0)	14 (12.5)	70 (62.5)

Kappa analysis κ=0.412, P<0.001; expressed as Spearman's correlation coefficient (ρ=0.834), P<0.001. AI-CACS, artificial intelligence-based coronary artery calcium score; ECG-CT CACS, electrocardiogram-gated computed tomography coronary artery calcium score.

Table 7 Confusion matrices of risk categories between the 1-mm AI-CACS group and 3-mm AI-CACS group

3-mm AI-CACS	1-mm AI-CACS, n				Total, n	Underestimation, n (%)	Overestimation, n (%)	Concordance, n (%)
	0	1–100	101–400	>400				
0	50	10	0	0	60	10 (16.7)	–	50 (83.3)
1–100	0	20	4	0	24	4 (16.7)	0	20 (83.3)
101–400	0	0	20	2	22	2 (9.1)	0	20 (90.9)
>400	0	0	1	5	6	–	1 (16.7)	5 (83.3)
Total	50	30	25	7	112	16 (14.3)	1 (0.9)	95 (84.8)

Kappa analysis κ=0.769, P<0.001; expressed as Spearman's correlation coefficient (ρ=0.916), P<0.001. AI-CACS, artificial intelligence-based coronary artery calcium score; ECG-CT CACS, electrocardiogram-gated computed tomography coronary artery calcium score.

1.0 and 3.0 mm; (II) the CACS calculated from the 1-mm slice width images derived from chest CT scans exhibited better performance the those calculated with 3- or 5-mm slice width images; and (III) The CACSs in the non-gated chest CT images were more likely to be underestimated or overestimated when the patients were evaluated as low-risk [1–100] CAD patients.

The Agatston score, which has been the most widely used method for quantifying CAC for more than three decades, remains a valuable tool in cardiovascular risk assessment. It aids in the early detection, risk stratification, treatment decision making, and monitoring of CAD progression in the current clinical landscape (7,30,31). To calculate the Agatston score precisely, the ECG-gated non-contrast enhanced cardiac CT scan procedure was developed to acquire images of the coronary arteries synchronized with the patient's heartbeat (32). However, our study showed that the CACS calculated from the chest CT scan using an AI-based algorithm had a good correlation with that of the standard ECG-gated cardiac CT scan, which supports the findings of previous studies (33,34).

Some studies (24,35) have calculated the CACSs using non-gated chest CT, but the studies did not further subdivide the image slice thickness, and were retrospective in nature. One study (36) analyzed the CACSs of chest CT scans with thicknesses of 1 and 3 mm, and found that the chest CT scans with a slice thickness of 3 mm were slightly more accurate in CAC detection and risk classification, which is inconsistent with our findings; however, our Kappa values for the risk classification of chest CT scans with a thicknesses of 1 mm were higher. A previous study (37) analyzed the CACSs of different slice thicknesses of electrocardiographic-gated cardiac CT scans. Unlike previous studies, the patients in our study were prospectively enrolled and underwent chest and ECG-gated CT scans sequentially. This approach allowed us to minimize the impact of factors introduced by variations in patients' conditions on different dates. Our study revealed that the CACSs calculated from images with a slice thickness of 1.0 mm, derived from chest CT scans showed no statistically significant differences and had the highest correlation of 0.973 when compared to the reference CACSs. However, the CACSs calculated

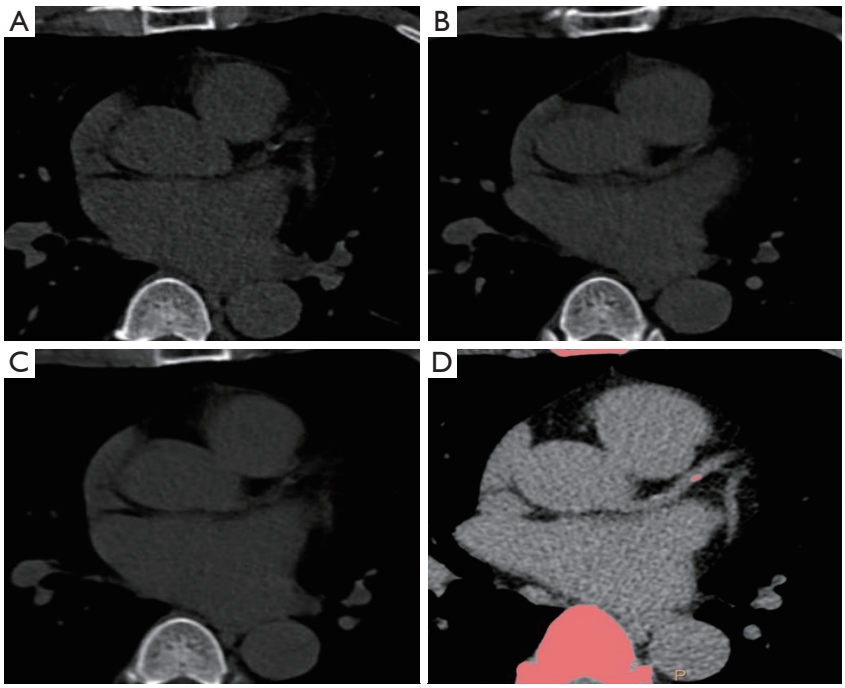

Figure 5 The CACS of a 59-year-old male. The ECG-CT CACS (D) was 4.03 with a low risk of CAD, and all the AI-CACSs of the chest CT scans with three different thicknesses (A: 1-mm AI-CACS, B: 3-mm AI-CACS, C: 5-mm AI-CACS) were 0 with a very low risk of CAD. (D) The red area of bone is not recorded in the CACS. CACS, coronary artery calcium score; ECG, electrocardiogram; CT, computed tomography; CAD, coronary artery disease; AI, artificial intelligence.

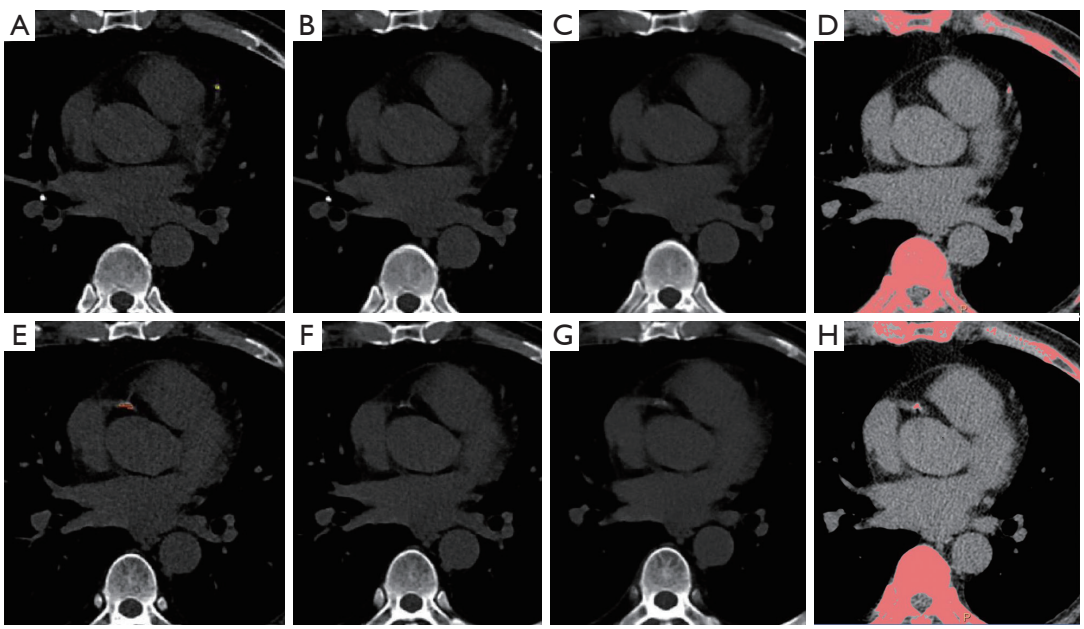

Figure 6 The CACS of a 61-year-old male. The ECG-CT CACS (D,H) was 20.25 and the 1-mm AI-CACS (A,E) was 48.91 with a low risk of CAD. However, the 3-mm AI-CACS (B,F) and 5-mm AI-CACS (C,G) were 0 with a very low risk of CAD. (D,H) The red area of bone is not recorded in the CACS. CACS, coronary artery calcium score; ECG, electrocardiogram; CT, computed tomography; CAD, coronary artery disease; AI, artificial intelligence.

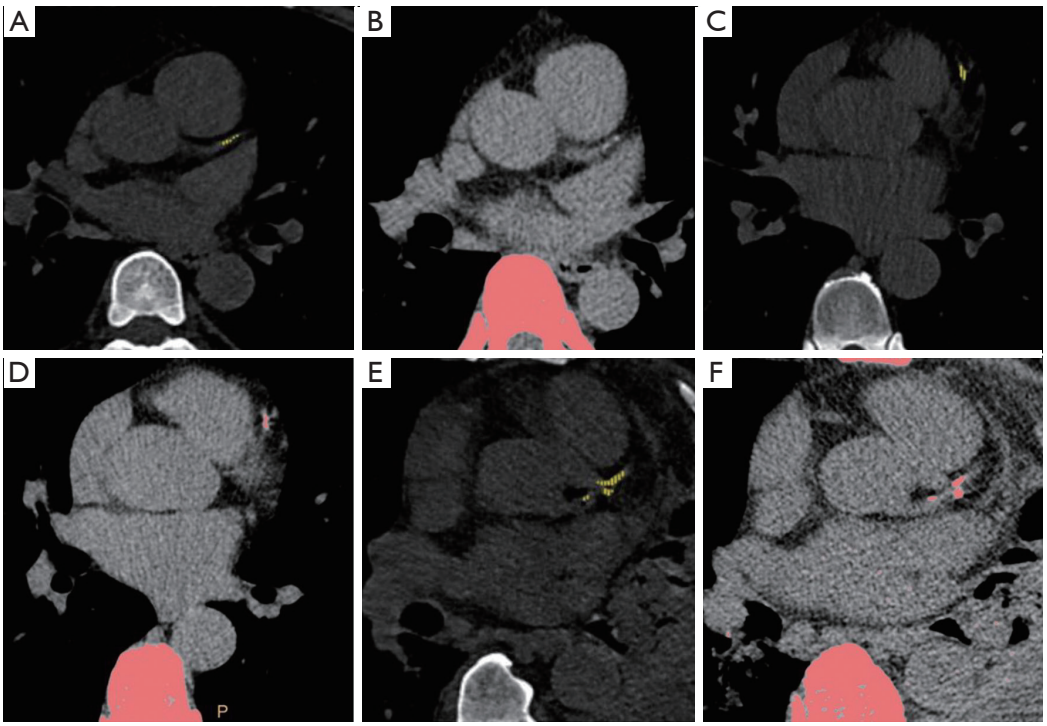

Figure 7 The CACS of a 54-year-old male. The ECG-CT CACS (B) was 0 with a very low risk of CAD, and the 1-mm AI-CACS (A) was 10.91 with a low risk of CAD. The CACS of a 60-year-old male (C,D). The ECG-CT CACS (D) was 68.02 with a low risk of CAD, and the 1-mm AI-CACS (C) was 137.13 with a moderate risk of CAD. The CACS of a 54-year-old male (E,F). The ECG-CT CACS (F) was 230.81 with a moderate risk of CAD, and the 1-mm AI-CACS (E) was 404.26 with a high risk of CAD. (B,D,F) The red area of bone is not recorded in the CACS. CACS, coronary artery calcium score; ECG, electrocardiogram; CT, computed tomography; CAD, coronary artery disease; AI, artificial intelligence.

from the other two slice thicknesses (3.0 and 5.0 mm) had significantly lower values.

The ECG-gated CT scan allowed us to acquire data during the diastolic phase of the cardiac cycle, which enabled us to measure calcium plaque accurately. However, the chest CT scan was not synchronized with ECG, which could potentially introduce calculation bias caused by cardiac motion. Further, the images with the thicker slice widths might be more affected by the volume effect, as a threshold of 130 HU was applied during the Agatston score calculation. Therefore, the 1.0-mm slice width images performed better for CACS measurements than the 3.0- and 5.0-mm slice width images, all of which were reconstructed from the same chest CT scan.

In a multi-center, multi-vendor retrospective study conducted by Xu *et al.*, the AI-CACS method from chest CT was compared with the manual method from cardiac CT. The study reported excellent correlation (ρ=0.893) and good agreement in risk categorization with a concordance rate of 80.6% (19). However, it should be noted that the chest CT images in that study had different slice widths, ranging from 0.625 to 5.0 mm, and the impact of image slice width on CACS results was not investigated. Our study showed that the AI-based CACS algorithm could provide more accurate results from chest CT images with a slice width of 1.0 mm. This shows the feasibility of calculating the CACSs for patients undergoing lung screening CT scans to predict the risk of CAD. However, our study also raised a concern that the AI-based algorithm may underestimate the risk of CAD, particularly in cases involving thick-slice chest CT images.

In terms of Agatston score-based risk categorization, the 1-mm AI-CACS group showed the highest accuracy at 91.0%, followed by the 3-mm AI-CACS group, which achieved an accuracy of 84.8%, using the ECG-CT CACS group as the reference. However, in the 5-mm AI-CACS group, only 62.5% of patients were categorized in the same risk category as the reference. The 5-mm AI-CACS group

significantly underestimated the risk with 77.8% (28/36) of patients categorized in group 1–100 being reclassified into group 0, 45.5% (10/22) of patients from group 101–400 being recategorized into group 1–100, and 57.1% (4/7) of patients in group >400 being reclassified into group 101–400 (*Table 6*).

It is well known that while a CAC score of 0 is associated with a very low prevalence of obstructive epicardial CAD and low event rates, it can also create a false sense of reassurance; therefore, the risk of CAD should not be completely ruled out (38). Further, the estimations from the 5-mm AI-CACS group could yield more false-negative results. The 3-mm AI-CACS group also exhibited this underestimation issue with 36.1% (13/36) of patients categorized in group 1–100 being reclassified into group 0. For the 1-mm AI-CACS group, only 11.1% (4/36) of the patients were reclassified into group 0. Our study also showed that 1-mm AI-CACS tended to overestimate the risk compared to the ECG-gated CACS group. Specifically, 2.1% (1/47) of patients categorized in group 0 were reclassified into group 1–100, 8.3% (3/36) of patients categorized in group 1–100 were reclassified into group 101–400, and 4.5% (1/22) of patients categorized in group 101–400 were reclassified into group >400 (*Figure 7*). Our study revealed that AI-CACS calculated from chest CT images with thinner slice widths (1.0 and 3 mm) were higher than those calculated from images with a slice width of 5 mm. Overall, the 1-mm AI-CACS group underestimated 4.4% (5/112) of patients and overestimated 4.4% (5/112) of patients, which closely aligned with the reference ECG-gated CACS group. Most of the underestimated cases belonged to the very low-risk group (CACS 0), while the overestimated cases were mainly distributed in the very low- to moderate-risk group (CACS 1–400). Of all the three AI-CACS groups, an underestimation or overestimation was most likely to occur in the evaluation of low-risk (CACS 1–100) CAD patients.

Our study had several limitations. First, the small sample size might have introduced selection bias. Second, we did not conduct separate statistical analyses on the CACSs of coronary artery branches. Third, all images were obtained from the same scanner at our hospital. Ultimately, we did not consider the potential impacts of varying tube voltages and patient heart rates on CACSs from non-gated chest CT scans. Therefore, we suggest that a larger multi-center, multi-vendor cohort study be conducted to address these limitations.

Conclusions

This prospective study showed the feasibility of using the proposed deep-learning method to automatically quantify the CACS from non-gated chest CT images. Our findings suggest that chest CT images with a slice width of 1 mm are suitable for CACS calculation and CAD risk stratification in patients undergoing lung screening.

Acknowledgments

The authors would like to thank the technicians and nursing teams at the Department of Radiology, Nanjing Drum Tower Hospital, The Affiliated Hospital of Nanjing University Medical School.

Funding: This study was supported by the National Natural Science Foundation of China (No. 82272065), the Medical Research Project of Jiangsu Health Commission in 2022 (No. M2022066), the Nanjing Medical Science and Technique Development Foundation (Nos. ZKX32019 and ZKX19018), the 15th Special Supported Project of China Postdoctoral Science Foundation (No. 2022T150317), the Nanjing Gulou Hospital New Technology Development Fund (Nos. XJSFZJJ202026 and XJSFZLX202114), and the Characteristic Project of Combined TCM and West Medicine Nanjing Drum Tower Hospital (No. CZXM2022106).

Footnote

Reporting Checklist: The authors have completed the STROBE reporting checklist. Available at https://qims.amegroups.com/article/view/10.21037/qims-24-247/rc

Conflicts of Interest: All authors have completed the ICMJE uniform disclosure form (available at https://qims.amegroups.com/article/view/10.21037/qims-24-247/coif). X.C. is an employee of Philips Healthcare. The other authors have no conflicts of interest to declare.

Ethical Statement: The authors are accountable for all aspects of the work in ensuring that questions related to the accuracy or integrity of any part of the work are appropriately investigated and resolved. The study was conducted in accordance with the Declaration of Helsinki (as revised in 2013). The study was approved the Institutional Ethics Committee of the Drum Tower Hospital, Medical

School of Nanjing University (No. 2022-547-01), and informed consent was obtained from all the patients.

References

1. Roth GA, Johnson C, Abajobir A, Abd-Allah F, Abera SF, Abyu G, et al. Global, Regional, and National Burden of Cardiovascular Diseases for 10 Causes, 1990 to 2015. J Am Coll Cardiol 2017;70:1-25.
2. Arnett DK, Blumenthal RS, Albert MA, Buroker AB, Goldberger ZD, Hahn EJ, Himmelfarb CD, Khera A, Lloyd-Jones D, McEvoy JW, Michos ED, Miedema MD, Muñoz D, Smith SC Jr, Virani SS, Williams KA Sr, Yeboah J, Ziaeian B. 2019 ACC/AHA Guideline on the Primary Prevention of Cardiovascular Disease: Executive Summary: A Report of the American College of Cardiology/American Heart Association Task Force on Clinical Practice Guidelines. J Am Coll Cardiol 2019;74:1376-414.
3. Sachdeva R, Valente AM, Armstrong AK, Cook SC, Han BK, Lopez L, et al. ACC/AHA/ASE/HRS/ISACHD/SCAI/SCCT/SCMR/SOPE 2020 Appropriate Use Criteria for Multimodality Imaging During the Follow-Up Care of Patients With Congenital Heart Disease: A Report of the American College of Cardiology Solution Set Oversight Committee and Appropriate Use Criteria Task Force, American Heart Association, American Society of Echocardiography, Heart Rhythm Society, International Society for Adult Congenital Heart Disease, Society for Cardiovascular Angiography and Interventions, Society of Cardiovascular Computed Tomography, Society for Cardiovascular Magnetic Resonance, and Society of Pediatric Echocardiography. J Am Coll Cardiol 2020;75:657-703.
4. Chiles C, Duan F, Gladish GW, Ravenel JG, Baginski SG, Snyder BS, DeMello S, Desjardins SS, Munden RF; . Association of Coronary Artery Calcification and Mortality in the National Lung Screening Trial: A Comparison of Three Scoring Methods. Radiology 2015;276:82-90.
5. Greenland P, Bonow RO, Brundage BH, Budoff MJ, Eisenberg MJ, Grundy SM, Lauer MS, Post WS, Raggi P, Redberg RF, Rodgers GP, Shaw LJ, Taylor AJ, Weintraub WS; . ACCF/AHA 2007 clinical expert consensus document on coronary artery calcium scoring by computed tomography in global cardiovascular risk assessment and in evaluation of patients with chest pain: a report of the American College of Cardiology Foundation Clinical Expert Consensus Task Force (ACCF/AHA Writing Committee to Update the 2000 Expert Consensus Document on Electron Beam Computed Tomography) developed in collaboration with the Society of Atherosclerosis Imaging and Prevention and the Society of Cardiovascular Computed Tomography. J Am Coll Cardiol 2007;49:378-402.
6. Du Y, Li Q, Sidorenkov G, Vonder M, Cai J, de Bock GH, et al. Computed Tomography Screening for Early Lung Cancer, COPD and Cardiovascular Disease in Shanghai: Rationale and Design of a Population-based Comparative Study. Acad Radiol 2021;28:36-45.
7. Agatston AS, Janowitz WR, Hildner FJ, Zusmer NR, Viamonte M Jr, Detrano R. Quantification of coronary artery calcium using ultrafast computed tomography. J Am Coll Cardiol 1990;15:827-32.
8. McEvoy JW, Blaha MJ, Nasir K, Blumenthal RS, Jones SR. Potential use of coronary artery calcium progression to guide the management of patients at risk for coronary artery disease events. Curr Treat Options Cardiovasc Med 2012;14:69-80.
9. Dickson JL, Horst C, Nair A, Tisi S, Prendecki R, Janes SM. Hesitancy around low-dose CT screening for lung cancer. Ann Oncol 2022;33:34-41.
10. Yip R, Jirapatnakul A, Hu M, Chen X, Han D, Ma T, Zhu Y, Salvatore MM, Margolies LR, Yankelevitz DF, Henschke CI. Added benefits of early detection of other diseases on low-dose CT screening. Transl Lung Cancer Res 2021;10:1141-53.
11. Šprem J, de Vos BD, Lessmann N, de Jong PA, Viergever MA, Išgum I. Impact of automatically detected motion artifacts on coronary calcium scoring in chest computed tomography. J Med Imaging (Bellingham) 2018;5:044007.
12. Liu Y, Chen X, Liu X, Yu H, Zhou L, Gao X, Li Q, Su S, Wang L, Zhai J. Accuracy of non-gated low-dose non-contrast chest CT with tin filtration for coronary artery calcium scoring. Eur J Radiol Open 2022;9:100396.
13. van Assen M, Martin SS, Varga-Szemes A, Rapaka S, Cimen S, Sharma P, Sahbaee P, De Cecco CN,

Vliegenthart R, Leonard TJ, Burt JR, Schoepf UJ. Automatic coronary calcium scoring in chest CT using a deep neural network in direct comparison with non-contrast cardiac CT: A validation study. Eur J Radiol 2021;134:109428.
14. Lee JG, Kim H, Kang H, Koo HJ, Kang JW, Kim YH, Yang DH. Fully Automatic Coronary Calcium Score Software Empowered by Artificial Intelligence Technology: Validation Study Using Three CT Cohorts. Korean J Radiol 2021;22:1764-76.
15. Chen L, Gu D, Chen Y, Shao Y, Cao X, Liu G, Gao Y, Wang Q, Shen D. An artificial-intelligence lung imaging analysis system (ALIAS) for population-based nodule computing in CT scans. Comput Med Imaging Graph 2021;89:101899.
16. Chetan MR, Dowson N, Price NW, Ather S, Nicolson A, Gleeson FV. Developing an understanding of artificial intelligence lung nodule risk prediction using insights from the Brock model. Eur Radiol 2022;32:5330-8.
17. Mu D, Bai J, Chen W, Yu H, Liang J, Yin K, Li H, Qing Z, He K, Yang HY, Zhang J, Yin Y, McLellan HW, Schoepf UJ, Zhang B. Calcium Scoring at Coronary CT Angiography Using Deep Learning. Radiology 2022;302:309-16.
18. Sandstedt M, Henriksson L, Janzon M, Nyberg G, Engvall J, De Geer J, Alfredsson J, Persson A. Evaluation of an AI-based, automatic coronary artery calcium scoring software. Eur Radiol 2020;30:1671-8.
19. Wang W, Wang H, Chen Q, Zhou Z, Wang R, Wang H, Zhang N, Chen Y, Sun Z, Xu L. Coronary artery calcium score quantification using a deep-learning algorithm. Clin Radiol 2020;75:237.e11-6.
20. Zeleznik R, Foldyna B, Eslami P, Weiss J, Alexander I, Taron J, et al. Deep convolutional neural networks to predict cardiovascular risk from computed tomography. Nat Commun 2021;12:715.
21. Lessmann N, van Ginneken B, Zreik M, de Jong PA, de Vos BD, Viergever MA, Isgum I. Automatic Calcium Scoring in Low-Dose Chest CT Using Deep Neural Networks With Dilated Convolutions. IEEE Trans Med Imaging 2018;37:615-25.
22. Xia C, Vonder M, Pelgrim GJ, Rook M, Xie X, Alsurayhi A, van Ooijen PMA, van Bolhuis JN, Oudkerk M, Dorrius M, van der Harst P, Vliegenthart R. High-pitch dual-source CT for coronary artery calcium scoring: A head-to-head comparison of non-triggered chest versus triggered cardiac acquisition. J Cardiovasc Comput Tomogr 2021;15:65-72.
23. Wolterink JM, Leiner T, de Vos BD, van Hamersvelt RW, Viergever MA, Išgum I. Automatic coronary artery calcium scoring in cardiac CT angiography using paired convolutional neural networks. Med Image Anal 2016;34:123-36.
24. Xu J, Liu J, Guo N, Chen L, Song W, Guo D, Zhang Y, Fang Z. Performance of artificial intelligence-based coronary artery calcium scoring in non-gated chest CT. Eur J Radiol 2021;145:110034.
25. Khursheed A, Hillier MC, Shrimpton PC, Wall BF. Influence of patient age on normalized effective doses calculated for CT examinations. Br J Radiol 2002;75:819-30.
26. Thomas IC, Forbang NI, Criqui MH. The evolving view of coronary artery calcium and cardiovascular disease risk. Clin Cardiol 2018;41:144-50.
27. Shemesh J, Henschke CI, Shaham D, Yip R, Farooqi AO, Cham MD, McCauley DI, Chen M, Smith JP, Libby DM, Pasmantier MW, Yankelevitz DF. Ordinal scoring of coronary artery calcifications on low-dose CT scans of the chest is predictive of death from cardiovascular disease. Radiology 2010;257:541-8.
28. Hutt A, Duhamel A, Deken V, Faivre JB, Molinari F, Remy J, Remy-Jardin M. Coronary calcium screening with dual-source CT: reliability of ungated, high-pitch chest CT in comparison with dedicated calcium-scoring CT. Eur Radiol 2016;26:1521-8.
29. Azour L, Kadoch MA, Ward TJ, Eber CD, Jacobi AH. Estimation of cardiovascular risk on routine chest CT: Ordinal coronary artery calcium scoring as an accurate predictor of Agatston score ranges. J Cardiovasc Comput Tomogr 2017;11:8-15.
30. Liaquat A, Khan A, Ullah Shah S, Iqbal H, Iqbal S, Rana AI, Ur Rahman H. Evaluating the use of coronary artery calcium scoring as a tool for coronary artery disease (CAD) risk stratification and its association with coronary stenosis and CAD risk factors: a single-centre, retrospective, cross-sectional study at a tertiary centre in Pakistan. BMJ Open 2022;12:e057703.
31. Huang W, Wong CJ. Performance of the coronary calcium score in an outpatient chest pain clinic and strategies for risk stratification. Clin Cardiol 2021;44:1189.
32. Vonder M, Vliegenthart R, Kaatee MA, van der Aalst CM, van Ooijen PMA, de Bock GH, Gratama JW, Kuijpers D, de Koning HJ, Oudkerk M. High-pitch versus sequential mode for coronary calcium in individuals with a high heart rate: Potential for dose reduction. J Cardiovasc Comput Tomogr 2018;12:298-304.
33. Yu J, Qian L, Sun W, Nie Z, Zheng D, Han P, Shi H,

Zheng C, Yang F. Automated total and vessel-specific coronary artery calcium (CAC) quantification on chest CT: direct comparison with CAC scoring on non-contrast cardiac CT. BMC Med Imaging 2022;22:177.
34. Andre F, Seitz S, Fortner P, Allmendinger T, Sommer A, Brado M, Sokiranski R, Fink J, Kauczor HU, Heussel CP, Herth F, Frey N, Görich J, Buss SJ. Simultaneous assessment of heart and lungs with gated high-pitch ultra-low dose chest CT using artificial intelligence-based calcium scoring. Eur J Radiol Open 2023;10:100481.
35. Yamamoto H, Fujimoto S, Aoshima C, Minamino T, Fujii T, Wakabayashi S, Urabe Y, Ueda H, Kunita E, Abe M, Higashino H. Feasibility of Simple Evaluation of Coronary Artery Calcium Using a Number of Chest Computed Tomography Slices: A Multicenter Study. Ann Vasc Dis 2023;16:46-53.
36. Xu C, Guo H, Xu M, Duan M, Wang M, Liu P, Luo X, Jin Z, Liu H, Wang Y. Automatic coronary artery calcium scoring on routine chest computed tomography (CT): comparison of a deep learning algorithm and a dedicated calcium scoring CT. Quant Imaging Med Surg 2022;12:2684-95.
37. Kim SY, Suh YJ, Lee HJ, Kim H, Seo H, Park HJ, Yang DH. Influence of computed tomography slice thickness on deep learning-based, automatic coronary artery calcium scoring software performance. Quant Imaging Med Surg 2023;13:4257-67.
38. Gottlieb I, Miller JM, Arbab-Zadeh A, Dewey M, Clouse ME, Sara L, Niinuma H, Bush DE, Paul N, Vavere AL, Texter J, Brinker J, Lima JA, Rochitte CE. The absence of coronary calcification does not exclude obstructive coronary artery disease or the need for revascularization in patients referred for conventional coronary angiography. J Am Coll Cardiol 2010;55:627-34.

Cite this article as: Yin K, Chen W, Qin G, Liang J, Bao X, Yu H, Li H, Xu J, Chen X, Wang Y, Savage RH, Schoepf UJ, Mu D, Zhang B. Performance assessment of an artificial intelligence-based coronary artery calcium scoring algorithm in non-gated chest CT scans of different slice thickness. Quant Imaging Med Surg 2024;14(8):5708-5720. doi: 10.21037/qims-24-247

